SLEEPJ, 2018, 1–13

doi: 10.1093/sleep/zsy130
Advance Access publication Date: 7 July 2018
Original Article

ORIGINAL ARTICLE

Characteristics of sleep-active neurons in the medullary parafacial zone in rats

Md. Aftab Alam[1,2], Andrey Kostin[1], Jerome Siegel[1,2], Dennis McGinty[1,3], Ronald Szymusiak[1,4] and Md. Noor Alam[1,4,*]

[1]Research Service (151A3), Veterans Affairs Greater Los Angeles Healthcare System, Sepulveda, CA, [2]Department of Psychiatry, University of California, Los Angeles, CA, [3]Department of Psychology, University of California, Los Angeles, CA and [4]Department of Medicine, David Geffen School of Medicine, University of California, Los Angeles, CA

*Corresponding author. Md. Noor Alam, Research Service (151A3), Veterans Affairs Greater Los Angeles Healthcare System, 16111 Plummer Street, Sepulveda, CA 91343. Email: noor@ucla.edu.

Abstract

Growing evidence supports a role for the medullary parafacial zone in non-rapid eye movement (non-REM) sleep regulation. Cell-body specific lesions of the parafacial zone or disruption of its GABAergic/glycinergic transmission causes suppression of non-REM sleep, whereas, targeted activation of parafacial GABAergic/glycinergic neurons reduce sleep latency and increase non-REM sleep amount, bout duration, and cortical electroencephalogram (EEG) slow-wave activity. Parafacial GABAergic/glycinergic neurons also express sleep-associated c-fos immunoreactivity. Currently, it is not clear if parafacial neurons are non-REM sleep-active and/or REM sleep-active or play a role in the initiation or maintenance of non-REM sleep. We recorded extracellular discharge activity of parafacial neurons across the spontaneous sleep-waking cycle using microwire technique in freely behaving rats. Waking-, non-REM sleep-, and REM sleep-active neuronal groups were segregated by the ratios of their discharge rate changes during non-REM and REM sleep versus waking and non-REM sleep versus REM sleep. Parafacial neurons exhibited heterogeneity in sleep-waking discharge patterns, but 34 of 86 (40%) recorded neurons exhibited increased discharge rate during non-REM sleep compared to waking. These neurons also exhibited increased discharge prior to non-REM sleep onset, similar to median preoptic nucleus (MnPO) and ventrolateral preoptic area (VLPO) sleep-active neurons. However, unlike MnPO and VLPO sleep-active neurons, parafacial neurons were weakly-moderately sleep-active and exhibited a stable rather than decreasing discharge across sustained non-REM sleep episode. We show for the first time that the medullary parafacial zone contains non-REM sleep-active neurons. These neurons are likely functionally important brainstem compliments to the preoptic-hypothalamic sleep-promoting neuronal networks that underlie sleep onset and maintenance.

Statement of Significance

Functional anatomical and chemogenetic studies support a role of the medullary parafacial zone in non-REM sleep regulation. We examined the discharge activity profiles of parafacial neurons across the spontaneous sleep-wake cycle. We confirmed the presence of neurons that are activated during non-REM sleep and/or REM sleep compared to waking. Discharge features of parafacial neurons during wake-sleep transition and during stable sleep episodes support the loss of function lesion studies and indicate a role for the parafacial zone in the initiation and maintenance of non-REM sleep. The neurotransmitters/neuromodulators and the mechanism that underlie sleep-wake dependent changes in the activity of parafacial neurons as well as interactions of these neurons with other sleep- and wake-promoting neuronal groups remain to be fully investigated.

Key Words: parafacial zone; median preoptic nucleus; ventrolateral preoptic area; extracellular recording; sleep-active neurons

Submitted: 19 February, 2018; **Revised:** 31 May, 2018

Introduction

Sleep is regulated by a network of sleep-active neuronal groups that are distributed at several levels of the neuraxis and through their interactions with circadian and wake-promoting neuronal networks [1–8]. GABAergic/glycinergic medullary neurons in a region of the parafacial zone localized dorsal to the facial nerve, have been implicated in the initiation and maintenance of sleep, especially non-rapid eye movement (non-REM) sleep [9]. Orexin-saporin immunotoxin-induced cell-body specific lesions of the parafacial zone in rats or genetic disruption of GABAergic/glycinergic transmission in the parafacial zone in mice produce sustained waking and suppression of non-REM sleep, even at the time of the day when sleep drive is strongest [10]. Conversely, genetically targeted activation of GABAergic/glycinergic neurons in this area reduce sleep latency and increase non-REM sleep amount, bout duration, and electroencephalogram (EEG) slow wave activity [11]. Findings on REM sleep are less consistent. While neurotoxic lesions of the parafacial zone do not affect REM sleep, both disruption of GABA/glycinergic transmission and activation of parafacial GABAergic/glycinergic neurons have been reported to decrease REM sleep [10, 11]. The evidence further suggests that parafacial zone contains neurons that express sleep-associated c-fos immunoreactivity (Fos-IR) and that >50% of those Fos-IR neurons are GABAergic/glycinergic [10]. Parafacial GABAergic neurons project to the wake-promoting parabrachial nucleus (PB) and potentially promote sleep and EEG slow wave activity by inhibiting the PB–basal forebrain-cortical circuitry [9, 11].

While the findings reviewed above suggest that neurons in the parafacial zone are activated during sleep, because of the poor temporal resolution of fos-expression as a marker of neuronal activity, it is not clear if these neurons are non-REM sleep-active and/or REM sleep-active or discharge in association with the initiation versus maintenance of non-REM sleep and/or REM sleep. The sleep-waking state discharge activity profiles of parafacial neurons in the sleep-promoting zone as identified by Anaclet and colleagues [10, 11] have not been described in freely behaving animals. This remains a fundamental knowledge gap regarding sleep regulatory functions of the parafacial zone.

Of various sleep-regulatory neuronal groups, sleep-active neurons localized in the ventrolateral preoptic area (VLPO) and median preoptic nucleus (MnPO) have been extensively studied using multiple approaches [1, 8, 12–17]. These neurons express the inhibitory neurotransmitters GABA and galanin (VLPO), project to major wake-promoting systems in the hypothalamus and brainstem and inhibit them to promote sleep [1, 8, 18–20]. The discharge profiles of MnPO and VLPO neurons and lesion studies suggest that these two neuronal groups play complementary roles in the onset and maintenance of sleep [13, 16, 21, 22]. A systematic comparison of discharge activity profiles of sleep-active parafacial neurons with those in the MnPO and VLPO may provide insights into the operation of these sleep-regulatory neuronal groups and their relative contributions in sleep-initiation or maintenance processes.

Here we describe the frequency and distribution of sleep-waking state discharge patterns of neurons recorded extracellularly within the parafacial zone as identified by Anaclet and colleagues [10, 11] to be a sleep-promoting region. Recorded neurons were classified by the ratios of their discharge during waking versus non-REM and REM sleep and non-REM sleep versus REM sleep to identify various subgroups of sleep- and waking-active neurons. We compared activity profiles of sleep-active parafacial neurons with sleep-active neurons in the MnPO and VLPO to determine similarities and differences in activity during waking to sleep transition and during stable sleep-waking states in those neuronal groups.

Methods

Experimental subjects

Experimental subjects were seven Sprague-Dawley male rats, weighing between 300 and 350 grams at the time of surgery. Rats were maintained on a 12:12-hour light-dark cycle (lights on at 08:30 am) and with food and water available ad libitum. All experiments were conducted in accordance with the National Research Council's "Guide for the Care and Use of Laboratory Animals," and procedures were reviewed and approved by the Institutional Animal Care and Use Committee of the Veterans Affairs Greater Los Angeles Healthcare System.

Surgical procedures

Under surgical anesthesia (Ketamine, 80 mg/kg + Xylazine, 10 mg/kg; IP) and aseptic conditions, rats were surgically prepared for chronic recording of extracellular neuronal activity in the parafacial zone as well as for the assessment of sleep-waking state. The details of the surgical and experimental procedures have been described previously [21, 23].

Briefly, EEG electrodes were threaded into the skull over the frontal and parietal cortices to record the EEG activity. Two Teflon-coated stainless steel wires, bared for 1–2 mm at the end, were implanted into the dorsal neck muscles to record the electromyogram (EMG). A single 23-gauge stainless-steel barrel attached to a mechanical microdrive was implanted stereotaxically (AP, -10.04; L, -1.5; and H, -4.00) such that its tip rested 2–3 mm dorsal to the parafacial zone [24]. Four pairs of microwires, each consisting of two 20 μm Formvar-insulated stainless steel microwires that were cut at an angle and glued together except for 2 mm at the tip, were passed through the barrel such that their tips protruded 2–3 mm beyond the tip of the cannula and into the parafacial zone. EEG and EMG electrodes, as well as microwires, were soldered to miniature plugs that were anchored to the skull with dental acrylic.

Data acquisition

Experiments were carried out after at least 10 days of recovery from surgery. During the recovery period, rats were placed in a cylindrical Plexiglas cage (Raturn System, United States) that was housed in a sound attenuated and electrically shielded chamber. Rats were acclimatized to the recording setup and recording cables for 2–3 hours during the last 2–3 days of the recovery period. In the recording chamber, rats were maintained at the same 12:12-hour light: dark cycle (illumination intensity about 100 lux) and had ad libitum access to food and water.

All electrophysiological recordings were performed on unrestrained and freely behaving rats between 09:00 am and 03:00 pm, during the light-phase. EEG and EMG signals were recorded using a Grass Model 78 polygraph, United States. Extracellular discharge activity from parafacial zone was recorded using bipolar derivations from microwires that were amplified by a

differential AC amplifier (model 1700, A-M System, Carlsborg, United States) and filtered between 10 Hz and 10 kHz. The microdrive was advanced in 15–30 μm steps until amplified microwire signals, as confirmed in oscilloscopic traces, showed the presence of action potential signals with signal: noise ratio ≥2.0. After each microdrive advancement, all microwires were systematically scanned during waking and non-REM sleep to ensure detection of both wake- and sleep-active neuronal types. All neuronal recordings that met the signal:noise criterion and yielded stable recordings across three or more complete sleep-wake cycles were analyzed and reported.

EEG, EMG, and unit signals were digitized using a Power1401 data acquisition interface and the Spike-2 Software (Cambridge Electronic Design, Cambridge, UK). Individual action potentials were sorted from filtered, amplified microwire recordings by spike shape parameters using the Spike-2 software. Spike-2 software produced templates based on waveform amplitude and shape for each distinct action potential present in the raw signal, and sorted action potentials throughout the recording by matching them with the templates. Spike shapes were based on 135 analog to digital sampling points. All spikes that did not match existing templates were stored for subsequent off-line examination to ensure that spikes were not incorrectly rejected. The discharge rate of each discriminated parafacial neuron was recorded through 3–5 stable sleep-wake cycles. After completion of these recordings, the microdrive was advanced again for isolating/recording additional units for the study. This sequence was repeated 2–3 times during a 6-hour recording period.

Histology

After recording all cells along the dorsoventral aspect of the targeted parafacial zone, rats were deeply anesthetized with pentobarbital (100 mg/kg, IP). First, microlesion was made at the tip of the microwire that yielded the highest number of cells by passing DC current (20 μA, 15–20 s) for plotting anatomical localization of the recorded neurons. Rats were then injected with heparin (500U, I.P.), and perfused transcardially with phosphate buffered saline (PBS; PH 7.4) followed by fixative containing 4% paraformaldehyde in PBS. The brains were removed, post-fixed, coronally cut at the 40 μm thickness and stained for Nissl bodies (Cresyl violet). The microwire tracts were histologically identified, and the locations of recorded neurons were reconstructed along each track with the aid of a Neurolucida image system (Microbrightfield, Colchester, VT). Since individual microwire pairs in a bundle could be separated by a maximum of 125 μm in laterality, depth or the anterior-posterior plane, the reconstructed locations of recorded neurons are subject to this potential error. Sections through the parafacial zone from other experimental animals were immunostained with GAD-67 antibody using standard protocol [22] to validate the distribution of GABAergic neurons in the parafacial zone in rats (Figure 1).

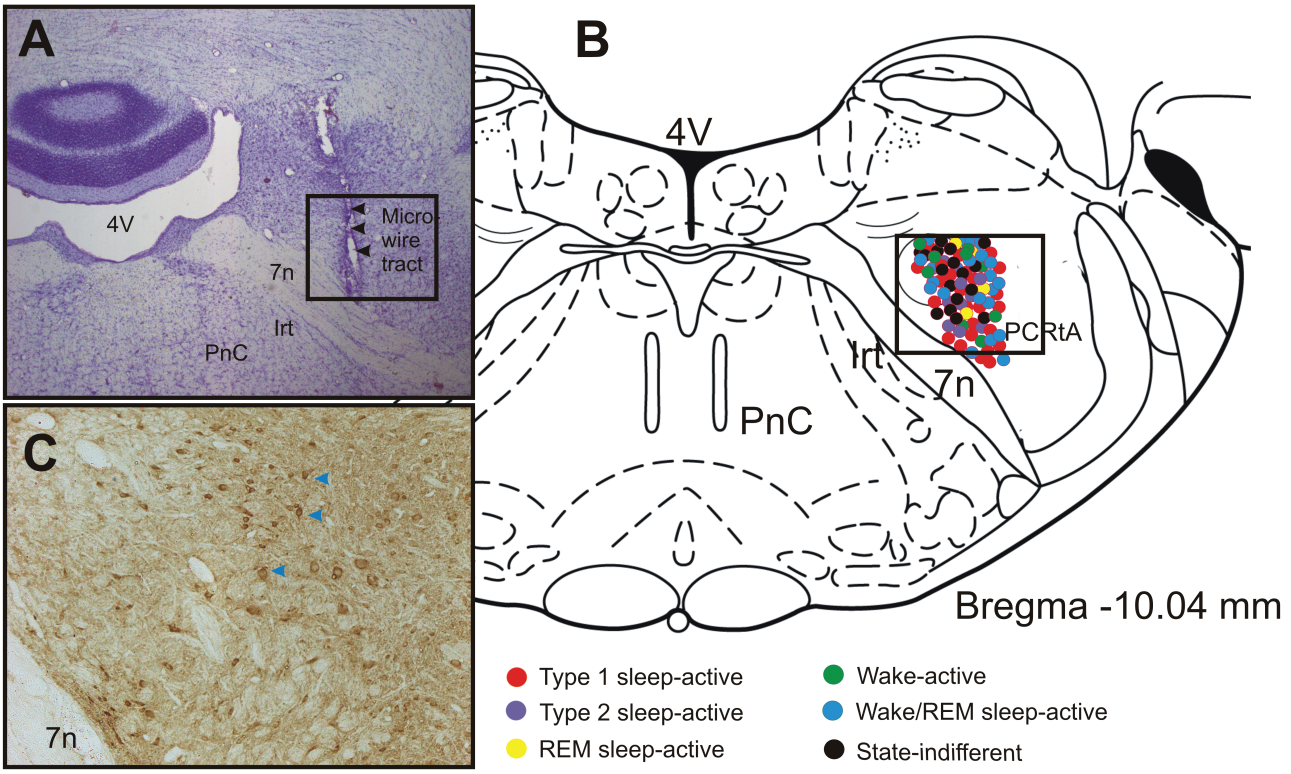

Figure 1. Site of extracellular recording and anatomical distribution of various sleep-wake neuronal phenotypes. (A). Photomicrograph of a representative coronal section (Nissl stained) through the parafacial zone showing the microwire tracts indicated by arrows. (B) Drawing of a representative coronal section through the parafacial zone [24] showing the anatomical distribution of the extracellularly recorded neurons along with their sleep-wake discharge profiles. Although, the rostro-caudal plane of the recorded neurons varied by 100–250 μm through the parafacial zone, they have been superimposed on a single plane of section for simplicity. (C) Photomicrograph of a representative coronal section through the parafacial zone showing the distribution of GAD67-immunopositive neurons (brown cells, arrows) in a comparable area as marked in figures (A) and (B). ●, type 1 sleep-active neurons; ●, type 2 sleep-active neurons; ●, REM sleep-active neurons; ●, wake active neurons; ●, wake/REM sleep-active neurons; and ●, state-indifferent neurons. Note that most of the recorded neurons were localized in the GABA-immunopositive neuronal field. 7n, facial nerve; 4V, fourth ventricle; IRt, Intermediate reticular nucleus; PCRtA, parvicellular reticular nucleus, alpha part; PnC, pontine reticular nucleus.

Data analysis

To determine changes in discharge of the recorded neurons across sleep-wake states, states of waking, non-REM sleep, and REM sleep were identified by EEG and EMG parameters using standard criteria [21, 23]. The mean discharge rate (±SEM) of neurons in waking, non-REM sleep, and REM sleep were calculated from 3 to 5 episodes of each state ranging in duration from 30 s to >300 s. Our review of the extracellular discharge indicated that recorded parafacial neurons exhibited several types of sleep-wake discharge patterns.

To segregate neurons by their waking, non-REM sleep, and REM sleep discharge profiles, we used non-REM sleep/wake, REM sleep/wake, and non-REM sleep/REM sleep discharge ratios and a minimum of 25% between-state discharge rate change criterion (see Table 1) [13, 21]. Neurons were classified as *sleep-active*, if non-REM sleep/wake discharge ratio was >1.25. Among sleep-active neurons, neurons were classified as *type 1 sleep-active*, if non-REM sleep/REM sleep discharge ratio was <1.25 and *type 2 sleep-active*, if non-REM sleep/REM sleep ratio was >1.25. Neurons were classified as *wake-active*, if non-REM sleep/wake and REM sleep/wake ratios were <0.75; *wake/REM sleep-active*, if non-REM sleep/wake ratio was <0.75 and REM sleep/wake ratio was between >0.75 and <1.25. Neurons exhibiting 25%–50%, >50%–100%, and >100% change were classified as weakly, moderately, and strongly state-related, respectively [13]. For classification of REM sleep-active neurons, a much stricter criterion was used. Neurons were classified as REM sleep-active if REM sleep/wake and REM sleep/ non-REM sleep ratios were >2.0. Neurons exhibiting non-REM sleep/wake and REM sleep/wake discharge ratios of >0.75 and <1.25 were classified as *state-indifferent* neurons.

To determine changes in discharge during waking to sleep transitions, mean discharge for each neuron during three episodes of entire waking (except for the last 10 s), during last 10 s before the first synchronization, and first 10 s of sleep-onset were compared (Figure 8). For determining time-dependent changes during non-REM sleep, non-REM sleep from the same sleep-waking episodes were divided into four quartiles (the first representing the early phase of non-REM sleep including sleep-onset and the fourth representing the last phase of non-REM sleep), and the discharge during each quartile was compared (Figure 2, Table 2).

The spike-2 software used for data acquisition and analysis effectively tracked and captured individual action potential across the sleep-wake state (Figures 3–8). However, the mean duration of each discriminated action potential for comparison was calculated from the averaged waveform, based on all the action potentials recorded during 2 minutes of stable sleep, using standard criterion [25, 26]. Action potential duration was measured from the initial inflection point from the baseline, positive peak, first zero crossing, negative peak, and second zero crossing.

Statistical analysis

The SigmaPlot (Systat Software, San Jose, CA) software package was used for statistical analysis of the data. For normally distributed data, effects of the sleep-waking state, waking to non-REM sleep transition, as well as time-dependent changes within non-REM sleep (four quartiles) on the discharge rate of each group of parafacial neurons were assessed with a one-way repeated measures analysis of variance (RM ANOVA) followed by Holm-Sidak test. When normality test failed, Friedman RM

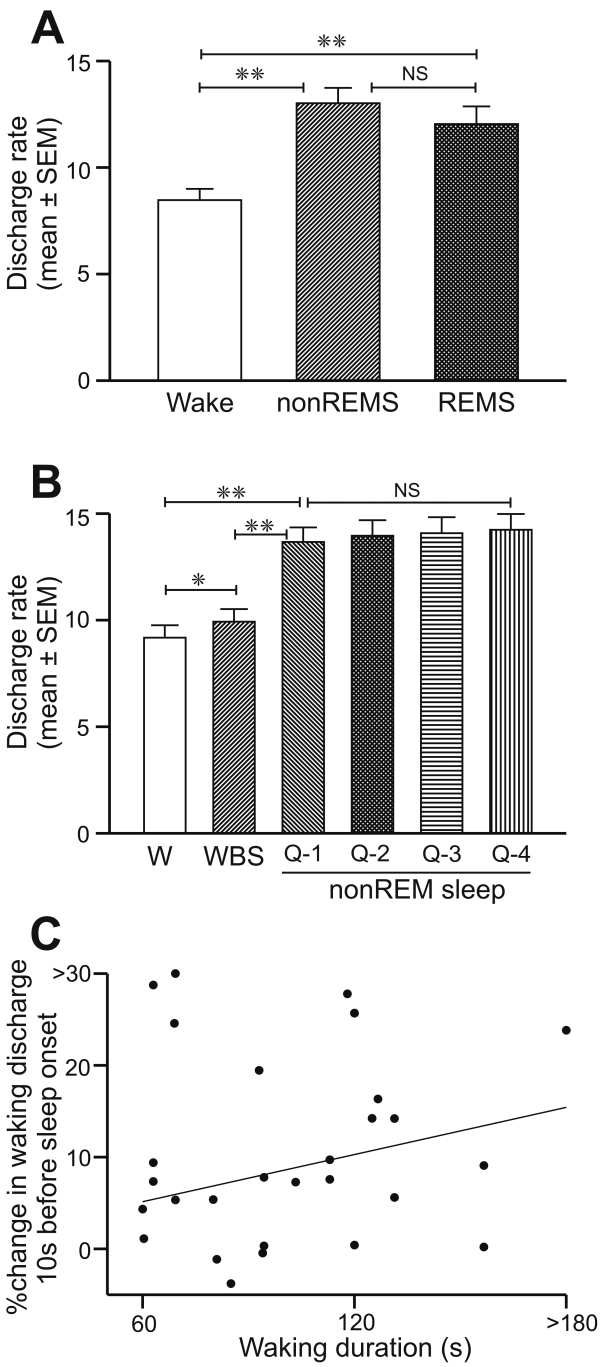

Figure 2. Discharge characteristics of sleep-active neurons. (A) Mean discharge rate (±SEM) of parafacial sleep-active neurons during waking, non-REM sleep and REM sleep. (B) Mean discharge rate (±SEM) of sleep-active neurons during waking to non-REM sleep transition (i.e. during waking and during the last 10 s of waking preceding non-REM sleep onset) and during the four quartiles of non-REM sleep. Note that these neurons exhibited increased discharge activity during the last 10 s of waking preceding sleep onset and a stable discharge rate across non-REM sleep episode including at its onset (first quartile) and termination (last quartile). (C) Percent change in discharge rate (mean) of individual neurons during the last 10 s of waking before sleep onset, as compared to prior waking discharge during the waking episode, plotted against waking episode duration (mean). The straight line in the graph represents simple linear regression between %change in discharge during the transition and duration of the waking episode. The percent increase in discharge rate during the last 10 s of waking was not significantly correlated with the waking bout duration. W, waking; WBS, last 10 s of waking before sleep-onset; Q, quartiles; s, second; $^{**}p < 0.01$; $^{*}p < 0.05$; NS, not significantly different.

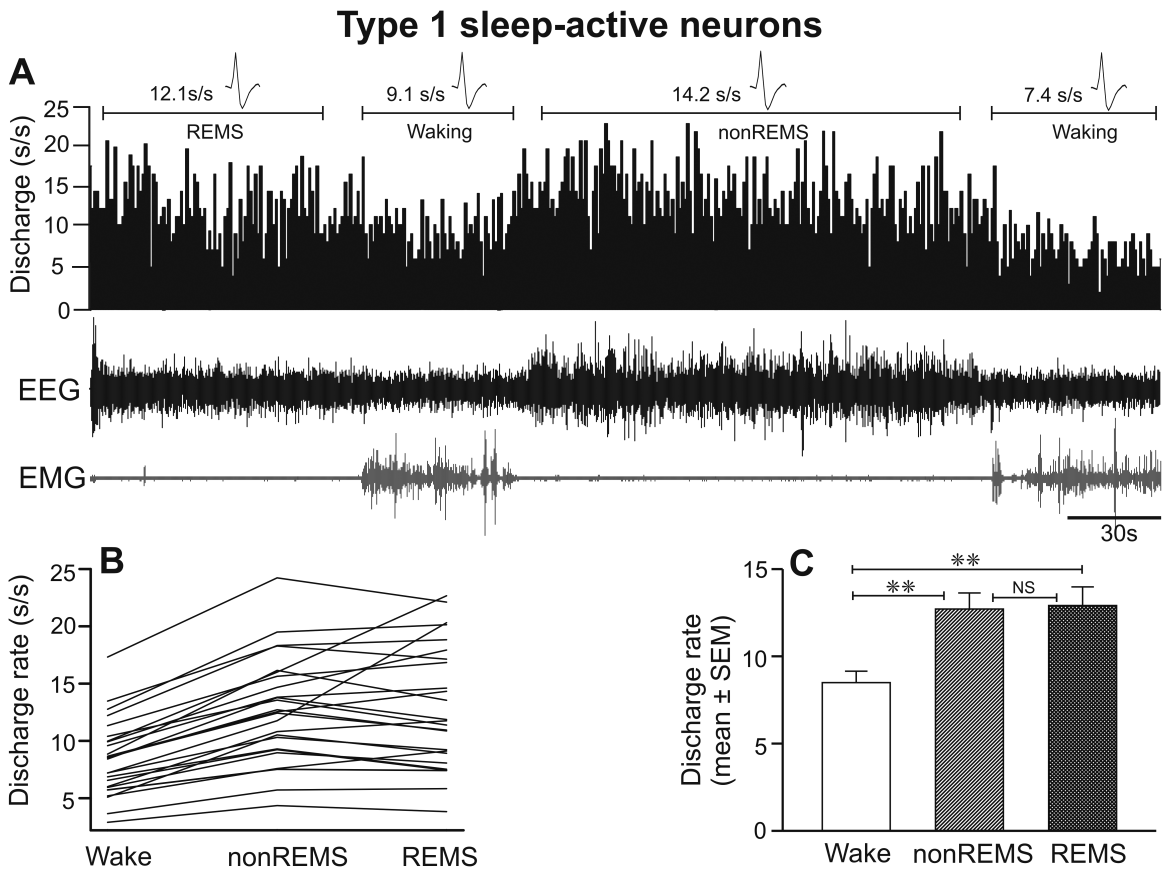

Figure 3. Discharge characteristics of type 1 sleep-active neurons. (A) A computer-generated 5-minute tracing, showing continuous discharge of an individual type 1 sleep-active neuron across sleep-wake cycle. Individual discharge rates of all the recorded neurons of this type and their mean discharge rate during waking, non-REM sleep, and REM sleep are shown in figures (B) and (C), respectively. The numbers on the top of the marked area represent mean discharge rate during the representative sections of the tracing. The spikes represent averaged waveforms of the action potentials captured during the marked sections and indicate that the same neuron was recorded across the sleep-waking state. These neurons as a group exhibited significantly higher discharge rates during both non-REM sleep and REM sleep, compared to waking. EEG, electroencephalogram; EMG, neck electromyogram; s/s, spikes/second; $^{**}p < 0.01$; NS, not significantly different.

ANOVA on ranks followed by Tukey test was used. The discharge rate changes and spike duration of type 1 and type 2 sleep-active neurons were compared using *t*-test (normal distribution) or Mann-Whitney Rank Sum Test when normality test failed. The discharge rates during waking, last 10 s of waking immediately preceding non-REM sleep onset and during the initial sleep-onset period, and spike durations for sleep-active parafacial, MnPO, and VLPO neurons were compared using One Way ANOVA followed by Holm-Sidak test or Kruskal-Wallis one-way ANOVA followed by Dunn's method, if normality test failed.

Results

Anatomical distribution of recorded neurons

A total of 86 neurons were recorded within the dorsal to ventral extent of the parafacial zone and characterized by their sleep-waking state discharge patterns in six out of seven rats. In one rat, the extracellular neuronal activity could not be recorded due to microdrive failure. Figure 1 shows representative histological sections through the parafacial zone showing microwire tracts (Figure 1A), anatomical localization of all recorded neurons with symbols indicating their sleep-waking discharge profiles (Figure 1B), as well as the distribution of GABAergic neurons in this area (Figure 1C). The various sleep-waking neuronal groups recorded in this study did not show clear anatomical segregation and were distributed in an area lateral to the genu of the facial nerve and dorsal to the facial nerve including the peritrigeminal zone and parvicellular reticular nucleus. This area also contained GAD67-immunopositive (GABAergic) neurons (Figure 1C).

Sleep-waking discharge profiles of parafacial neurons

The 86 neurons encountered in the parafacial zone exhibited heterogeneous sleep-waking discharge patterns and high discharge variability within each state. Overall, there was a significant effect of sleep-waking states on the discharge frequency of parafacial neurons as a group ($F = 9.934$; $p < 0.001$). The mean discharge rate of the recorded neurons during REM sleep (12.92 ± 0.63 spikes/s) was significantly higher than the mean discharge rate during waking (11.22 ± 0.59 spikes/s) as well as during non-REM sleep (10.98 ± 0.55 spikes/s). The discharge rates during waking and non-REM sleep were not significantly different ($p > 0.05$). However, based on the percent change in discharge rates during non-REM sleep compared to waking as well as non-REM sleep versus REM sleep, parafacial neurons were classified into sleep-active (40%), REM sleep-active (5%), wake/REM sleep-active (24%), wake-active (10%), and state-indifferent (21%) neurons. The discharge characteristics of these neuronal groups are described below.

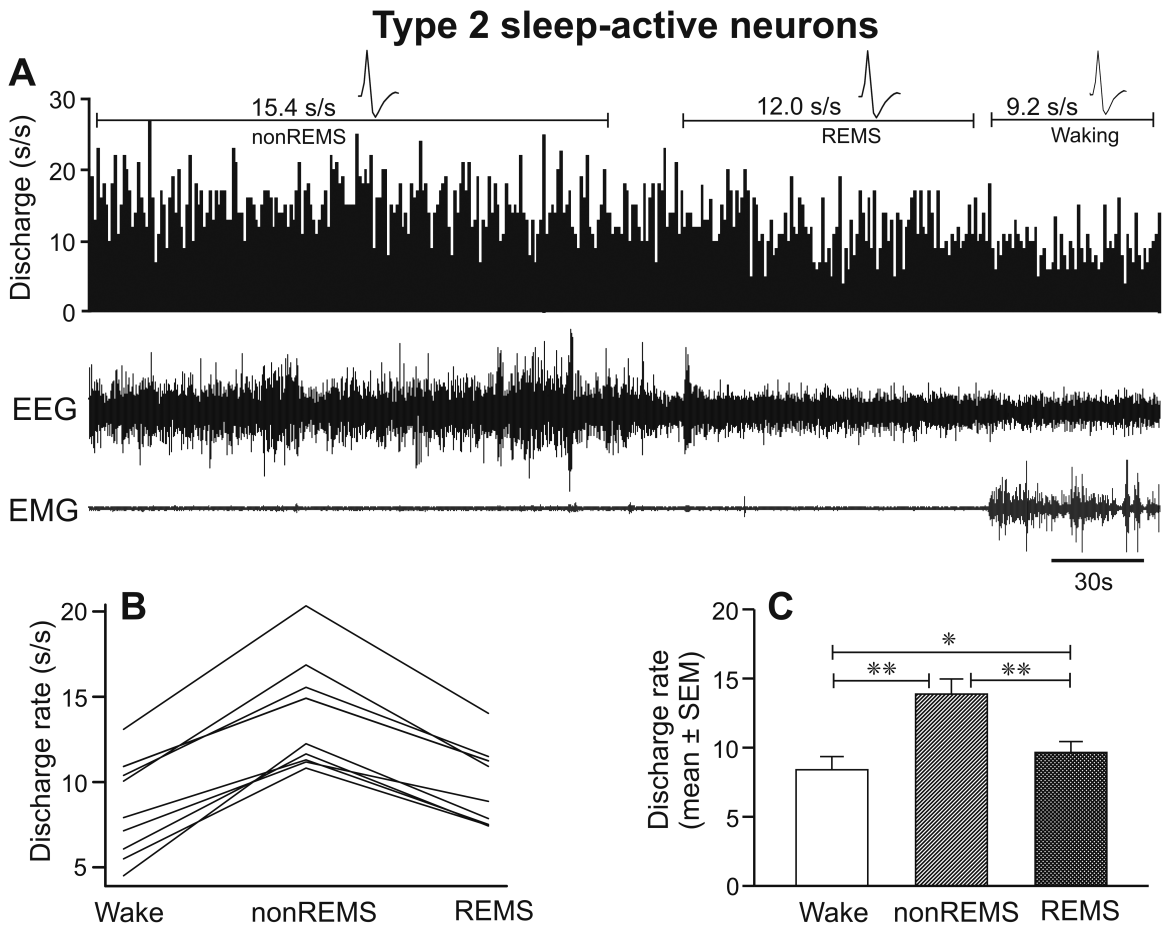

Figure 4. Discharge characteristics of type 2 sleep-active neurons. (A) A 5-minute continuous recording, showing the discharge activity of an individual type 2 sleep-active neuron across sleep-wake cycle. Individual discharge rates (B) and mean discharge rate of all the recorded neurons as a group (C) during waking, non-REM sleep, and REM sleep. These neurons as a group exhibited a significantly higher discharge rate during non-REM sleep, compared to both waking and REM sleep. Abbreviations are same as in Figure 3. $^{*}p < 0.05$; $^{**}p < 0.01$.

Sleep-active neurons

This was the most commonly encountered neuronal type (34 of 86 sampled neurons). The mean discharge activity of sleep-active neurons as a group in sleep-waking states, during waking to non-REM sleep transition, and in four quartiles of sustained non-REM sleep episode are shown in Figure 2 (A–C).

There were significant effects of sleep-waking state changes (chi-square = 50.529; $p < 0.001$; Figure 2A) and waking to non-REM sleep transitions ($F = 196.268$; $p < 0.001$; Figure 2B) on the discharge activity of these neurons. Sleep-active neurons, as a group, exhibited lowest discharge rate during waking, which increased significantly during the last 10 s of waking immediately preceding EEG sign of non-REM sleep onset (Figure 2B). This increase was not correlated with prior waking duration (Figure 2C). The discharge rate increased further with non-REM sleep onset. Within sustained non-REM sleep, the discharge rate of these neurons during first (or initial phase), second, third, and fourth (termination of non-REM sleep) quartiles did not differ significantly ($p > 0.05$; Figure 2B). As a group, these neurons exhibited comparable discharge activity during non-REM sleep and REM sleep (Figure 2A). While most sleep-active neurons in the parafacial zone exhibited increased discharge during both non-REM sleep and REM sleep compared to waking, 9 of 34 discharged at higher rates during non-REM sleep compared to both REM sleep and waking. The state-dependent discharge of the two subtypes of sleep-active neurons (type 1 and type 2) are described below.

Type 1 sleep-active neurons

Of 34 sleep-active neurons, 25 (74%) were classified as type 1. The spontaneous discharge activity of a typical type 1 sleep-active neuron across the spontaneous sleep-waking cycle, the individual discharge rate of all the recorded neurons of this type, as well as mean discharge rate as a group during waking, non-REM sleep, and REM sleep are shown in Figure 3 (A–C) and Tables 1 and 2.

These neurons exhibited increased and similar discharge rates during both non-REM sleep and REM sleep, compared to waking ($F = 44.805$, $p < 0.001$). Within non-REM sleep, discharge rates during first, second, third, and fourth quartiles were comparable ($p > 0.05$; Table 2). Based on the percentage increase in discharge rate during non-REM sleep compared to waking, 16 neurons were identified as weakly (25%–50%), eight as moderately (>50%–100%), and one as strongly (>100%) sleep-active.

Type 2 sleep-active neurons

Nine of 34 sleep-active neurons (26%) were identified as type 2. The continuous discharge of a typical type 2 neuron across the sleep-waking cycle, the individual discharge rates of all the recorded type 2 neurons and mean group discharge rates in

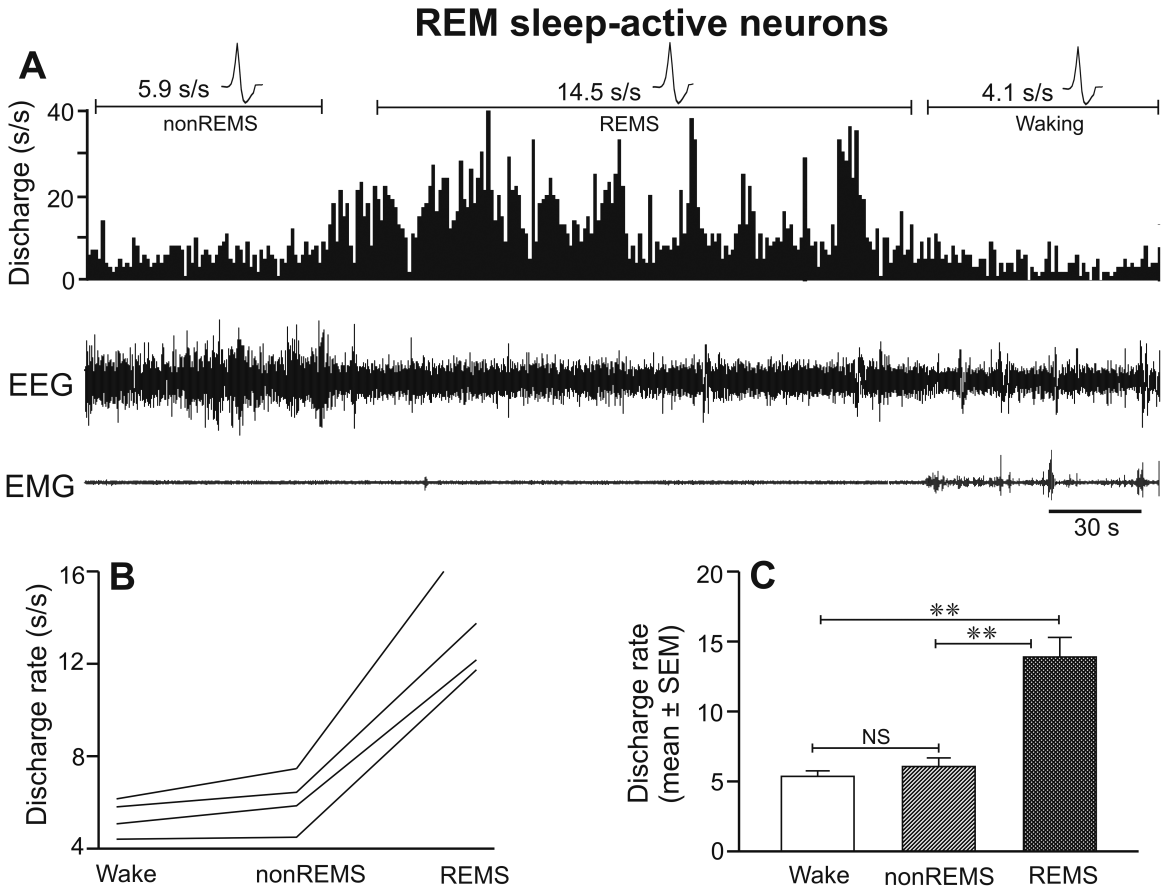

Figure 5. Discharge characteristics of REM sleep-active neurons. (A) A computer-generated 5-minute tracing showing the discharge of an individual REM sleep-active neuron across sleep-wake cycle. Individual discharge rates (spikes/second) of all the recorded REM sleep-active neurons and their mean discharge rate (±SEM) as a group during waking, non-REM sleep, and REM sleep are shown in figures (B) and (C), respectively. These neurons as a group exhibited significantly higher discharge during REM sleep, compared to both waking and non-REM sleep. Abbreviations are same as in Figure 3.

waking, non-REM sleep, and REM sleep are shown in Figure 4 (A–C) and Tables 1 and 2.

These neurons exhibited significantly higher discharge during non-REM sleep, compared to both waking and REM sleep ($F = 88.84$, $p < 0.001$). These neurons also exhibited comparable discharge activity across first, second, third, and fourth quartiles of the sustained non-REM sleep episode ($p > 0.05$; Table 2). The discharge rate during REM sleep was significantly higher than the mean discharge in waking (20 ± 8%; $p < 0.05$). Based on the percentage increase in discharge rate during non-REM sleep compared to waking, 3, 5, and 1 neurons were identified as weakly, moderately, and strongly sleep-active, respectively.

A comparison between discharge characteristics of type 1 and type 2 sleep-active neurons are shown in Tables 1 and 2. It is pertinent to note that except for significant difference in percent change in REM sleep compared to non-REM sleep (1 ± 4 vs. –30 ± 2%, $p < 0.001$), type 1 and type 2 sleep-active neurons exhibited similar discharge characteristics, including (1) comparable discharge frequencies in waking and non-REM sleep ($p > 0.05$), (2) significantly higher discharge rates in REM sleep than waking; (3) comparable percent increases during waking to sleep transitions ($p > 0.05$); and (4) comparable discharge rate changes during the first, second, third, and fourth quartiles of non-REM sleep episode ($p > 0.05$). The action potential durations of these two neuronal groups were also comparable ($p > 0.05$). These similarities suggest that the potential sleep-regulatory functions of the two neuronal types are similar, and therefore for comparisons with preoptic-hypothalamic sleep-active neuronal activity (see later), they are combined.

REM sleep-active neurons

REM sleep-active neurons were the least frequently encountered sleep-active neuronal type and constituted 11% of the sleep-active neuronal group (four out of 38 sleep-active neurons) or 5% of the sampled population. The sleep-waking profiles of the REM sleep-active neurons are shown in Figure 5 (A–C) and Table 1. These neurons exhibited highest discharge activity during REM sleep, which was significantly higher than their discharge rates during waking as well as non-REM sleep ($F = 65.778$; $p < 0.001$). Based on the percentage increase in discharge as compared to waking and non-REM sleep, all of the recorded neurons were classified as strongly REM sleep-active. Waking and non-REM sleep discharge rates of these neurons were not significantly different ($p > 0.05$).

Wake/REM sleep-active neurons

This was the most frequently encountered wake-active neuronal type. Of 86 recorded neurons, 21 neurons (24%) were identified as wake/REM sleep-active type. Computer generated tracings showing the discharge pattern of a typical wake/REM sleep-active neuron across the spontaneous sleep-wake cycle, the individual discharge rate of all the recorded neurons and

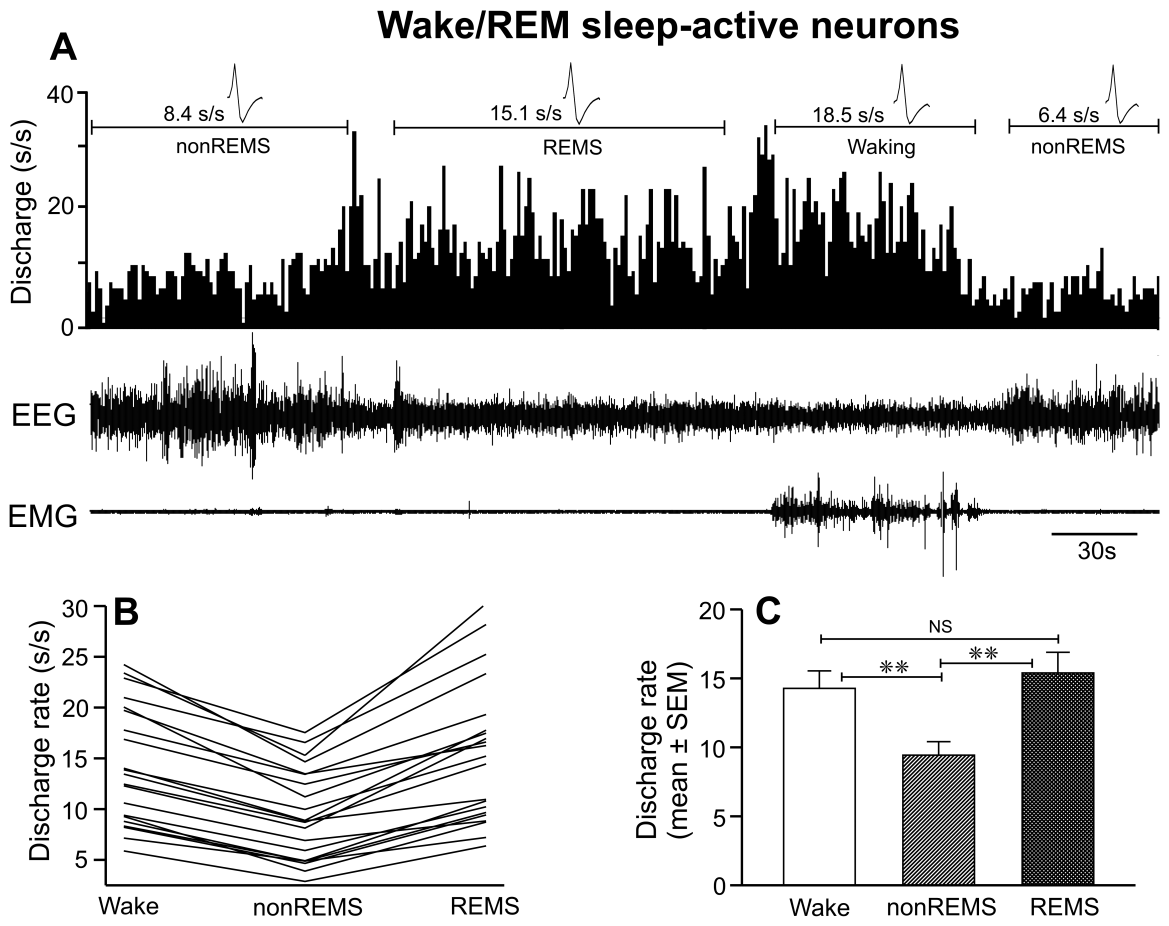

Figure 6. Discharge characteristics of wake/REM sleep-active neurons. (A) A 5-minute recording showing the discharge of an individual wake/REM sleep-active neuron across sleep-wake cycle. Individual discharge rates of all the recorded wake/REM sleep-active neurons and their mean discharge rate during waking, non-REM sleep, and REM sleep are shown in figures (B) and (C), respectively. These neurons as a group exhibited significantly higher discharge activity during both waking and REM sleep compared to non-REM sleep. Abbreviations are same as in Figure 3.

their mean discharge rate during waking, non-REM sleep and REM sleep are shown in Figure 6 (A–C) and Table 1.

There was a significant effect of sleep-waking state changes on the discharge activity of neurons in this group ($F = 59.313$; $p < 0.001$). As a group, these neurons exhibited minimal discharge activity during non-REM sleep and comparable discharge rates during waking and REM sleep ($p > 0.05$). As compared to non-REM sleep, these neurons exhibited significantly higher discharge activity during waking (36% ± 2%) as well as in REM sleep (71% ± 7%). Except for two neurons (>50%), all neurons exhibited only 25%–50% decrease in discharge activity during non-REM sleep as compared to waking or were weakly wake/REM sleep-active.

Wake-active neurons

Wake-active neurons constituted 10% ($n = 9$) of the recorded neuronal population. The real-time sleep-waking discharge profile of a typical wake-active neuron across sleep-wake cycle and their individual, as well as mean discharge rates during waking, non-REM sleep, and REM sleep, are shown in Figure 7 (A–C) and Table 1.

There was a significant effect of sleep-waking state on the discharge rate of these neurons ($F = 23.363$; $p < 0.001$). These neurons exhibited maximal discharge during waking and significantly decreased discharge in non-REM sleep (–56% ± 3%) and REM sleep (–41% ± 2%). The discharge rates during non-REM sleep and REM sleep were comparable ($p > 0.05$). Based on their non-REM sleep/waking ratio, two neurons were weakly, and seven neurons were moderately wake-active.

Unlike wake-active monoaminergic, histaminergic, and hypocretinergic neurons, wake-active neurons in the parafacial zone exhibited relatively higher discharge frequency across sleep-waking states and did not exhibit near cessation of activity in REM sleep [27–29].

State-indifferent neurons

Eighteen of 86 recorded neurons (21%) exhibited a less than 25% change in their discharge activity across sleep-waking states and were considered as state-indifferent neurons (Table 1).

Comparison of sleep-active neurons in the parafacial zone and preoptic area

Previous studies indicate that parafacial zone is involved in the regulation of sleep, especially non-REM sleep [10, 11]. In this study, we found that sleep-active neurons were the most common cell type in the parafacial zone. Such sleep-active neurons also constitute predominant groups in the MnPO and VLPO of the preoptic-hypothalamic region [12–14].

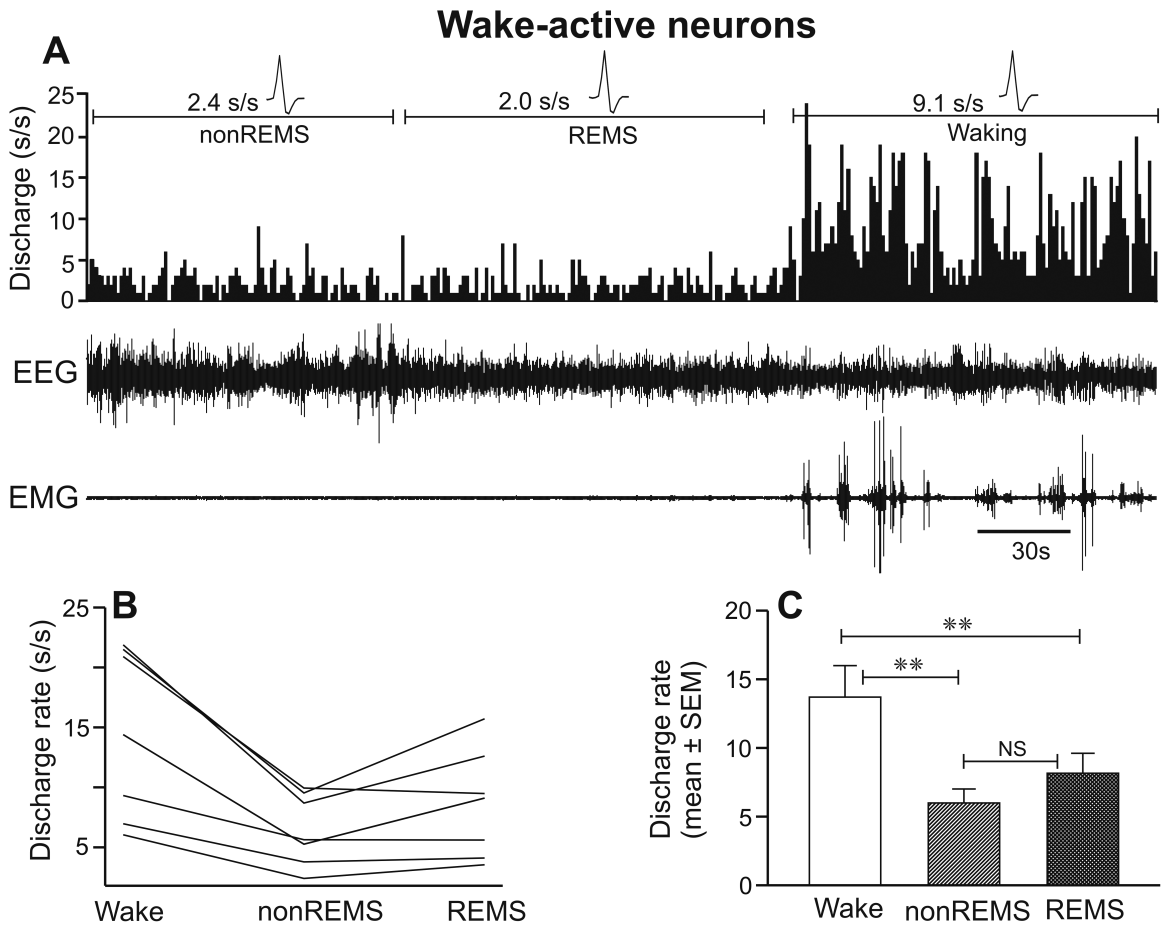

Figure 7. Discharge characteristics of wake-active neurons. (A) A 5-minute recording showing the discharge of an individual wake-active neuron across sleep-wake cycle. Individual discharge rates of all the recorded wake-active neurons (B) and their mean discharge rate as a group (C) during waking, non-REM sleep, and REM sleep. These neurons as a group exhibited a significantly higher discharge during waking, compared to both non-REM sleep and REM-sleep. Abbreviations are same as in Figure 3.

We compared discharge activity of 34 sleep-active parafacial neurons with those recorded in the MnPO ($n = 12$) and VLPO ($n = 14$) during the course of waking to non-REM sleep transition, to determine if these neuronal groups differ in their physiological response to sleep-onset. We re-analyzed sleep-wake discharge profiles of MnPO and VLPO neurons during transition using same neurons (11 MnPO and 13 VLPO neurons) that were studied for their responses to sleep deprivation in an earlier study [21]. Two additional cells, one each for MnPO and VLPO that could not be studied during sleep deprivation in the earlier study have also been included in this comparison with medullary neurons. The spontaneous discharge activity of individual sleep-active parafacial, MnPO, and VLPO neurons across waking to non-REM sleep transition and their mean discharge rate as a group during waking, last 10 s of the waking epoch immediately preceding EEG synchronization, and during 10 s of sleep-onset are shown in Figure 8 (A–F) and Table 3.

Compared to VLPO and MnPO neurons, spontaneous discharge frequency of parafacial sleep-active neurons was significantly higher during waking ($F = 17.798$, $p < 0.001$), during the last 10 s of waking epoch preceding sleep onset ($F = 15.864$, $p < 0.001$) and during the first 10 s of sleep onset ($F = 22.139$, $p < 0.001$; Table 3).

During sustained waking, in all three neuronal groups, discharge increased significantly during the last 10-s epoch preceding sleep onset, as compared to the discharge during the prior waking period. The magnitude of increase in parafacial neurons was not significantly different from those exhibited by MnPO and VLPO sleep-active neurons ($p > 0.05$; Table 3).

At non-REM sleep onset, the discharge rates of sleep-active neurons increased further compared to the discharge rates during the last 10-s epoch preceding sleep onset in all three neuronal groups. The magnitude of this increase for sleep-active parafacial neurons was not significantly different from those exhibited by sleep-active MnPO ($p > 0.05$) and VLPO ($p > 0.05$) neurons (Table 3).

The mean action potential duration of sleep-active parafacial neurons was not significantly different from the action potential duration of sleep-active neurons in the MnPO ($p > 0.05$). The action potential duration of sleep-active VLPO neurons, however, was significantly longer compared to that exhibited by parafacial neurons ($p < 0.05$; Table 3).

Conclusion/Discussion

We found that 44% of the sampled parafacial neurons exhibited increased discharge rate in one or both phases of sleep compared to waking. This population included neurons that were more active during both non-REM sleep and REM sleep compared to waking and those that were active more selectively during non-REM sleep. A few were more selectively active in

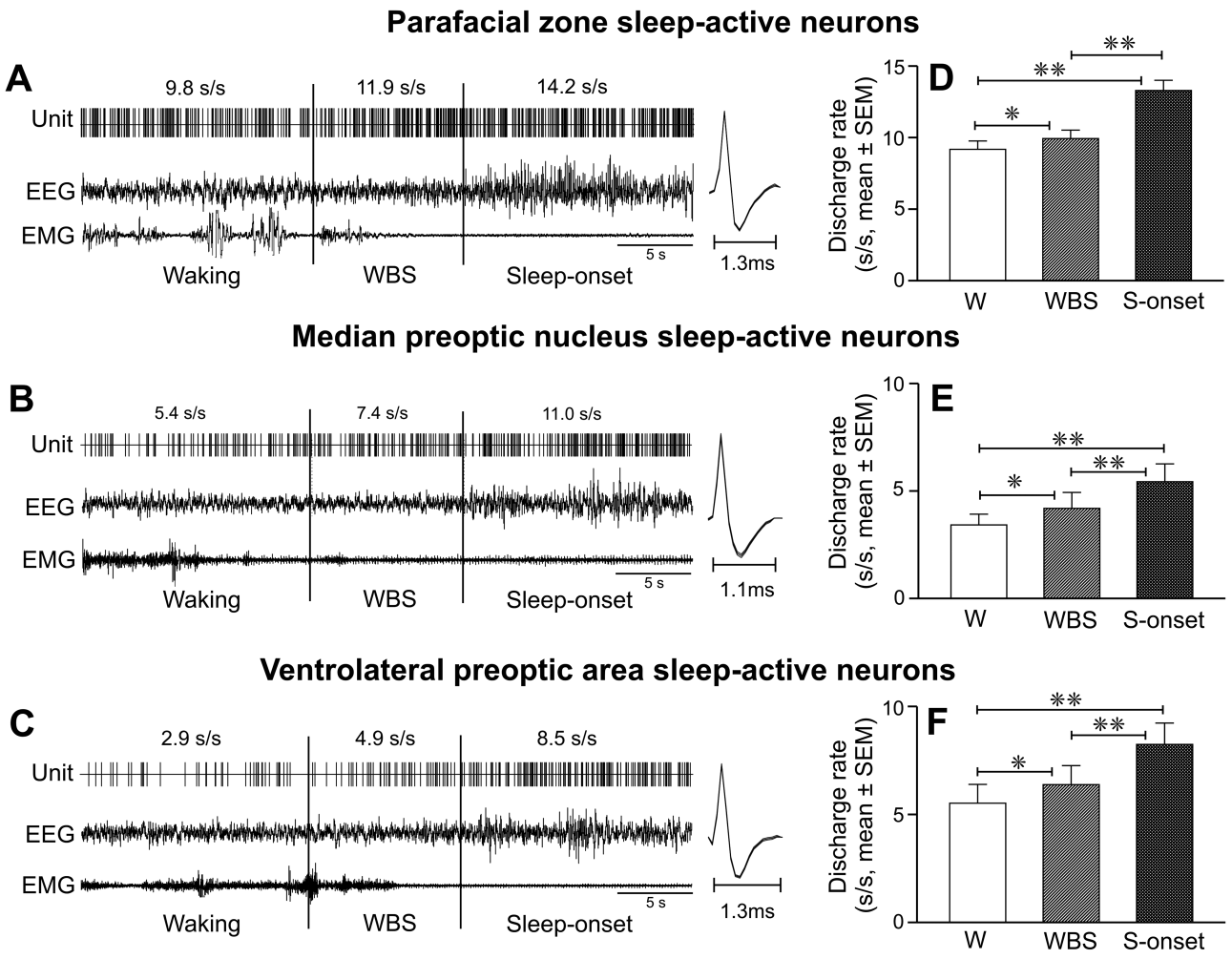

Figure 8. Discharge changes in parafacial zone, MnPO, and VLPO sleep-active neurons during waking to non-REM sleep transition. (A–C) Computer generated continuous tracing showing discharge activity of individual sleep-active parafacial zone, MnPO, and VLPO neurons during 15 s of waking, last 10 s of waking immediately preceding EEG synchronization, and during 15 s of sleep onset. The spikes on the side represent averaged waveforms of all the action potentials captured during the presented recording period. (D–F) Mean discharge rates of sleep-active parafacial zone, MnPO, and VLPO neurons during waking (except for the last 10 s), during the last 10 s of waking before sleep-onset, and during first 10 s of non-REM sleep onset. Note that all three neuronal groups exhibited increased discharge within 10 s prior to EEG synchronization and sleep-onset. Abbreviations are same as in Figures 2 and 3.

REM sleep. Parafacial zone sleep-active neurons exhibited higher spontaneous discharge rate compared to those recorded from both MnPO and VLPO. Parafacial sleep-active neurons become activated during waking prior to non-REM sleep onset, like MnPO and VLPO neurons. However, unlike MnPO and VLPO sleep-active neurons, parafacial neurons exhibited a stable rather than decreasing discharge across sustained non-REM sleep episode.

The present study is the first characterization of the extracellular discharge profiles of parafacial neurons across spontaneous sleep-wake cycle in freely behaving rats. Based on our reconstructions of the microwire tracts, all 86 neurons that are described in this study were localized in an area dorsal to the facial nerve including the peritrigeminal zone and parvicellular reticular nucleus, a region that also contained GAD-67 immunopositive neurons (Figure 1). These sleep-active neurons were intermingled with other sleep-wake neuronal types in the region and did not show anatomical segregation. GABAergic/glycinergic neurons exhibiting sleep-associated Fos-IR are also distributed throughout this region of the parafacial zone [10]. The prevalence of sleep-active neurons in the parafacial zone is consistent with a role of this medullary region in the regulation of one or more components of sleep.

Recent studies suggest that activation/inactivation of GABAergic/glycinergic neurons in the parafacial zone promotes and suppresses non-REM sleep and delta activity, respectively, and that parafacial GABAergic/glycinergic neurons exhibit sleep-associated Fos-IR [10, 11]. Based on these findings, one would predict that neurons exhibiting non-REM sleep-related discharge activity would be a common cell type within regions of the parafacial zone, where Fos-IR in GABAergic/glycinergic neurons is elevated during sleep. Here we report that non-REM sleep-active neurons were the most commonly encountered neuronal type in the parafacial zone. We also note that the extracellular recording method employed in this study precludes identification of the neurotransmitter phenotype of recorded neurons, it is likely that at least some of the recorded sleep-active neurons were GABAergic. However, given that (1) only ~50% parafacial GABAergic/glycinergic neurons exhibit sleep-associated Fos-IR[10]; (2) within the parafacial zone GABAergic neurons are

Table 1. Sleep-waking discharge characteristics of neurons in the parafacial zone

Neuronal group	Total (%)	Mean discharge rate (±SEM)			Mean discharge ratio (±SEM)		
		Waking	non-REM sleep	REM sleep	non-REMS/wake	REMS/wake	non-REMS/REMS
1. Type 1 sleep-active neurons	25 (29%)	8.49 ± 0.66 (2.89–17.32)	12.71 ± 0.92 (4.35–24.23)	12.91 ± 1.07 (3.83–22.66)	1.52 ± 0.03 (1.30–2.07)	1.43 ± 0.05 (1.10–1.96)	1.02 ± 0.03 (0.58–1.24)
2. Type 2 sleep-active neurons	9 (10%)	8.40 ± 0.96 (4.51–13.09)	13.87 ± 1.09 (10.82–20.33)	9.65 ± 0.79 (7.42–14.03)	1.74 ± 0.14 (1.37–2.72)	1.20 ± 0.08 (0.95–1.36)	1.45 ± 0.04 (1.33–1.57)
3. REM sleep-active neurons	4 (5%)	5.36 ± 0.39 (4.41–6.15)	6.06 ± 0.62 (4.49–7.46)	13.89 ± 1.40 (11.74–17.89)	1.12 ± 0.04 (1.02–1.21)	2.59 ± 0.13 (2.37–2.91)	0.44 ± 0.02 (0.38–0.48)
4. Wake-REM sleep-active neurons	21 (24%)	14.27 ± 1.27 (5.88–24.23)	9.43 ± 0.98 (2.88–17.53)	15.39 ± 1.50 (7.21–30.24)	0.64 ± 0.02 (0.42–0.75)	1.08 ± 0.04 (0.81–1.38)	0.61 ± 0.03 (0.45–0.83)
5. Wake-active neurons	9 (10%)	13.87 ± 2.14 (6.05–21.88)	5.79 ± 0.97 (2.40–9.95)	8.29 ± 1.37 (3.55–15.72)	0.42 ± 0.04 (0.28–0.60)	0.60 ± 0.02 (0.45–0.73)	0.72 ± 0.07 (0.45–1.05)
6. State-indifferent neurons	18 (21%)	12.84 ± 1.29 (4.40–24.82)	12.64 ± 1.32 (4.49–24.51)	13.78 ± 1.43 (4.57–24.36)	0.98 ± 0.03 (0.80–1.23)	1.07 ± 0.02 (0.84–1.27)	0.92 ± 0.03 (0.76–1.27)

Mean is based on 3–5 episodes of each state. Numbers in parenthesis denote range.

interspersed with other cell types, and (3) we encountered a relatively high percentage of sleep-active neurons, it is possible that non-REM sleep-active discharge pattern may not be specific to GABAergic neurons.

It is pertinent to note that our categorization of sleep-active neurons into type 1 and type 2 groups was based solely on the magnitude of changes in discharge activity in REM sleep compared to non-REM sleep. Otherwise, both of these neuronal groups exhibited comparable discharge frequencies in waking, the magnitude of increase in discharge in transition from waking to non-REM sleep and during sustained non-REM sleep (Table 2). The action potential durations of these two neuronal groups were also comparable (Table 2). Therefore, it is likely that the two neuronal groups are variations of the same neuronal phenotype and contribute similarly to or share one or more components of sleep regulatory function.

A recent study by Sakai [26] in head-restrained mice reported that none of the 125 recorded neurons in the parafacial zone exhibited tonically and/or selectively increased discharge activity during non-REM sleep or non-REM–REM sleep compared to waking. While there are methodological differences between our study and Sakai's, the discrepancy in findings on the prevalence of neurons with sleep-related discharge may be due to differences in the locations of the recorded neurons. Our recording sites were rostral and lateral to the genu of the facial nerve and dorsal to the nerve (Figure 1, A and B), a region closely aligned with the sleep-promoting region of the parafacial zone as defined by functional anatomical and chemogenetic studies [10, 11]. The majority of the recorded neurons in Sakai's study were localized lateral and ventral to our recording sites and included neurons located caudal to the genu of the facial nerve (Figure 2; Sakai [26]), including many neurons within the PCRt region which has been linked to phasic masseter muscle activity during REM sleep [30]. While the two studies differed in terms of recording electrode configuration (microwires vs. glass micropipettes), use of recording preparation (freely behaving vs. head restraint), and species (rats vs. mice), the minimal overlap in recordings sites is the most likely explanation for the differences in reported findings.

Sleep-active GABAergic neurons have been reported throughout the brain including in neocortex, basal forebrain, preoptic-anterior hypothalamic area, posterior lateral hypothalamus, zona incerta, and parafacial zone (see Introduction). We compared

Table 2. Activity profiles of type 1 and type 2 sleep-active neurons during waking to sleep transition and during non-REM sleep

Neuronal group	Type 1	Type 2
Number of neurons	25	9
Discharge rate, waking (s/s)	9.4 ± 0.6	8.5 ± 1.1
Discharge rate, last 10 s of waking (s/s)	10.2 ± 0.6	9.2 ± 1.0
%change compared to prior waking	9 ± 2	13 ± 8
Discharge rate, sleep onset (s/s)	13.2 ± 0.7	13.7 ± 1.3
%change compared to last 10 s of waking	32 ± 3	52 ± 8
Discharge rate, non-REM sleep episode (s/s)	14.0 ± 0.8	13.9 ± 1.1
non-REM sleep discharge (quartile 1)	13.6 ± 0.7	13.7 ± 1.0
non-REM sleep discharge (quartile 2)	14.0 ± 0.8	13.7 ± 1.0
non-REM sleep discharge (quartile 3)	14.1 ± 0.8	14.0 ± 1.1
non-REM sleep discharge (quartile 4)	14.3 ± 0.8	14.2 ± 1.1
Mean non-REM sleep episode duration(s)	420 ± 27	390 ± 62
Spike duration (ms)	1.22 ± 0.03	1.26 ± 0.03

s/s, spikes/second. Values are mean ± SEM.

sleep-wake discharge characteristics of parafacial sleep-active neurons with those localized in the MnPO and VLPO, neuronal groups with relatively well-characterized roles in sleep onset and maintenance [1, 8, 13, 14, 21]. We found that parafacial sleep-active neurons display significantly higher spontaneous discharge frequency across the sleep-waking state as compared to those in the MnPO and VLPO. The neurotransmitters/neuromodulators and the underlying mechanism(s) that modulates the spontaneous discharge rate changes of parafacial neurons across sleep-wake cycle remains poorly understood. However, like MnPO and VLPO sleep-active neurons, parafacial neurons also exhibited increased discharge several seconds before EEG defined non-REM sleep onset. This suggests that like MnPO and VLPO, parafacial sleep-active neurons play a role in the initiation of non-REM sleep.

Based on the non-REM sleep/waking discharge ratios, we found that parafacial zone not only contains lower number of sleep-active neurons compared to the MnPO (68%) and VLPO (56%), most of the parafacial neurons were weakly (19 of 34, 56%) to moderately (13 of 34, 38%) sleep-active [13, 14]. Only 6% were strongly sleep-active. Applying the same criteria, extracellular recording from MnPO and VLPO suggest that majority of neurons in these two regions are strongly sleep-active. Of 61 MnPO sleep-active neurons, 31 (51%) were strongly, and 25 (41%) were moderately sleep-active [13]. Amongst VLPO neurons, the majority of sleep-active

Table 3. Comparison of discharge activity of sleep-active neurons in the parafacial zone, median preoptic nucleus, and ventrolateral preoptic area during waking to sleep transition

Neuronal group	Parafacial zone	Ventrolateral preoptic area	Median preoptic nucleus
Number of neurons	34	14	12
Discharge rate waking (s/s)	9.2 ± 0.6*,†	5.5 ± 0.9	3.4 ± 0.5
Discharge rate, last 10 s of waking (s/s)	9.9 ± 0.6*,†	6.4 ± 0.9	4.2 ± 0.7
%change compared to waking	10 ± 3	22 ± 7	20 ± 7
Discharge rate, sleep onset (s/s)	13.3 ± 0.7*,†	8.2 ± 1.0	5.4 ± 0.8
%change compared to last 10 s of waking	34 ± 4	35 ± 6	41 ± 11
Spike duration (ms)	1.23 ± 0.02*	1.38 ± 0.03	1.30 ± 0.05

Values are mean ± SEM.
*Compared to the ventrolateral preoptic area.
†Compared to median preoptic nucleus.
**,†† <0.01; *,† < 0.05.

neurons (15 of 23 neurons, 65%) were also identified as strongly sleep-active [14]. This suggests that parafacial zone is less selectively active during non-REM sleep compared to waking. We only recorded parafacial neuronal activity during the light-phase, and it is possible that discharge of these neurons during waking reflects circadian modulation of sleep propensity. Characterization of the extent and nature of circadian influences on the activity of sleep-active parafacial neurons requires further study.

Another characteristic of MnPO and VLPO sleep-active neurons is that they exhibit a progressive decline in discharge rate during the course of a non-REM sleep episode, which parallels a decline in delta activity [13, 14, 21]. We found that parafacial sleep-active neurons exhibit stable discharge activity across non-REM sleep; their discharge rates do not differ significantly across four quartiles of sustained non-REM sleep episodes. Thus, the discharge of parafacial neurons is consistently elevated during stable, sustained non-REM sleep episodes and may not be responsive to changes in sleep depth. A systematic examination of parafacial zone neuronal activity at differing levels of homeostatic sleep drive, as we have reported for MnPO and VLPO neurons, has not been done [21].

The existence of a medullary sleep promoting system has long been inferred from studies conducted decades ago [9, 31, 32]. However, recent findings including the findings of this study confirm that this sleep-regulatory function likely emanates from a relatively delimited node of GABAergic/glycinergic parafacial neurons [10, 11]. Increased Fos-IR in parafacial GABAergic/glycinergic neurons as well as the relationships of parafacial neuronal discharge to sleep expression, especially non-REM sleep, as observed in this study, support a crucial role for parafacial neurons in sleep regulation. Recent studies suggest that sleep-active parafacial GABAergic/glycinergic neurons project to and exert inhibitory influences on wake-active PB neurons [9, 11]. PB neurons in turn project to and release synaptic glutamate onto cortically projecting magnocellular basal forebrain neurons that are tonically active during waking and function to promote EEG activation [2, 5, 33, 34]. We found that parafacial neurons were activated during waking to non-REM sleep transition and maintained elevated discharge rate during both non-REM sleep and REM sleep. Thus, via inhibitory modulation of PB-basal forebrain-cortical circuitry, these neurons may not only initiate sleep but also provide stability to sleep stages. The similar state-dependent discharge profiles of sleep-active cell types in the parafacial zone and the preoptic-hypothalamic area suggest that these systems exert comparable sleep-regulatory functions.

In summary, the findings of this study suggest that parafacial zone contains neurons exhibiting heterogeneous sleep-wake discharge profiles but that a majority are active in non-REM sleep. These neurons exhibit increased discharge several seconds before EEG defined non-REM sleep onset and exhibit sustained increase in discharge during entire non-REM sleep episode including at the onset and before the termination of non-REM sleep into waking or REM sleep. The neurotransmitters/neuromodulators and mechanism(s) underlying activation of these neurons during waking to sleep transition and during sleep, the response of these neurons to homeostatic or circadian influences, and the nature and extent of interactions between parafacial zone and other sleep-wake promoting systems including MnPO and VLPO remain to be fully investigated. Future studies using multipronged approaches including identifying neurotransmitter phenotypes of sleep-active neurons can address these critical questions. Our findings suggest that the physiological profile of parafacial sleep-active neurons resembles that of sleep-active preoptic-hypothalamic neurons to a large extent and that these neurons are functionally important brainstem components of inhibitory neuronal networks that underlie sleep onset and sleep maintenance, consistent with published functional anatomical and chemogenetic studies in rats and mice [9–11].

Funding

This work was supported by the US Department of Veterans Affairs, Merit Awards, BX000936 (Alam), BX003520 (McGinty), R01 DA034748, BX001753 (Siegel), and BX00155605 (Szymusiak).
Conflict of interest statement. None declared.

References

1. Alam MN. NREM sleep: anatomy and physiology. In *Encyclopaedia of Sleep*. Elsevier; 2013, 453–459.
2. Brown RE, *et al*. Control of sleep and wakefulness. *Physiol Rev*. 2012;**92**(3):1087–1187.
3. Gerashchenko D, *et al*. Identification of a population of sleep-active cerebral cortex neurons. *Proc Natl Acad Sci U S A*. 2008;**105**(29):10227–10232.
4. Hassani OK, *et al*. Discharge profiles of identified GABAergic in comparison to cholinergic and putative glutamatergic basal forebrain neurons across the sleep-wake cycle. *J Neurosci*. 2009;**29**(38):11828–11840.

5. Jones BE. Principal cell types of sleep-wake regulatory circuits. *Curr Opin Neurobiol*. 2017;**44**:101–109.
6. Konadhode RR, *et al*. Optogenetic stimulation of MCH neurons increases sleep. *J Neurosci*. 2013;**33**(25):10257–10263.
7. Liu K, *et al*. Lhx6-positive GABA-releasing neurons of the zona incerta promote sleep. *Nature*. 2017;**548**(7669):582–587.
8. Saper CB, *et al*. Sleep state switching. *Neuron*. 2010;**68**(6):1023–1042.
9. Anaclet C, *et al*. Brainstem regulation of slow-wave-sleep. *Curr Opin Neurobiol*. 2017;**44**:139–143.
10. Anaclet C, *et al*. Identification and characterization of a sleep-active cell group in the rostral medullary brainstem. *J Neurosci*. 2012;**32**(50):17970–17976.
11. Anaclet C, *et al*. The GABAergic parafacial zone is a medullary slow wave sleep-promoting center. *Nat Neurosci*. 2014;**17**(9):1217–1224.
12. Alam MN, *et al*. Neuronal discharge of preoptic/anterior hypothalamic thermosensitive neurons: relation to NREM sleep. *Am J Physiol*. 1995;**269**(5 Pt 2):R1240–R1249.
13. Suntsova N, *et al*. Sleep-waking discharge patterns of median preoptic nucleus neurons in rats. *J Physiol*. 2002;**543**(Pt 2):665–677.
14. Szymusiak R, *et al*. Sleep-waking discharge patterns of ventrolateral preoptic/anterior hypothalamic neurons in rats. *Brain Res*. 1998;**803**(1–2):178–188.
15. Sherin JE, *et al*. Activation of ventrolateral preoptic neurons during sleep. *Science*. 1996;**271**(5246):216–219.
16. Lu J, *et al*. Effect of lesions of the ventrolateral preoptic nucleus on NREM and REM sleep. *J Neurosci*. 2000;**20**(10):3830–3842.
17. Gong H, *et al*. Activation of c-fos in GABAergic neurones in the preoptic area during sleep and in response to sleep deprivation. *J Physiol*. 2004;**556**(Pt 3):935–946.
18. Sherin JE, *et al*. Innervation of histaminergic tuberomammillary neurons by GABAergic and galaninergic neurons in the ventrolateral preoptic nucleus of the rat. *J Neurosci*. 1998;**18**(12):4705–4721.
19. Kumar S, *et al*. Inactivation of median preoptic nucleus causes c-Fos expression in hypocretin- and serotonin-containing neurons in anesthetized rat. *Brain Res*. 2008;**1234**:66–77.
20. Uschakov A, *et al*. Sleep-active neurons in the preoptic area project to the hypothalamic paraventricular nucleus and perifornical lateral hypothalamus. *Eur J Neurosci*. 2006;**23**(12):3284–3296.
21. Alam MA, *et al*. Neuronal activity in the preoptic hypothalamus during sleep deprivation and recovery sleep. *J Neurophysiol*. 2014;**111**(2):287–299.
22. Gvilia I, *et al*. Homeostatic regulation of sleep: a role for preoptic area neurons. *J Neurosci*. 2006;**26**(37):9426–9433.
23. Alam MA, *et al*. Glutamic acid stimulation of the perifornical-lateral hypothalamic area promotes arousal and inhibits non-REM/REM sleep. *Neurosci Lett*. 2008;**439**(3):281–286.
24. Paxinos G, *et al*. *The Rat Brain in Stereotaxic Coordinates*. 4th ed. San Diego, CA: Academic Press; 1998.
25. Alam MN, *et al*. Sleep-waking discharge patterns of neurons recorded in the rat perifornical lateral hypothalamic area. *J Physiol*. 2002;**538**(Pt 2):619–631.
26. Sakai K. Are there sleep-promoting neurons in the mouse parafacial zone? *Neuroscience*. 2017;**367**:98–109.
27. Lee MG, *et al*. Discharge of identified orexin/hypocretin neurons across the sleep-waking cycle. *J Neurosci*. 2005;**25**(28):6716–6720.
28. Guzmán-Marín R, *et al*. Discharge modulation of rat dorsal raphe neurons during sleep and waking: effects of preoptic/basal forebrain warming. *Brain Res*. 2000;**875**(1-2):23–34.
29. Steininger TL, *et al*. Sleep-waking discharge of neurons in the posterior lateral hypothalamus of the albino rat. *Brain Res*. 1999;**840**(1–2):138–147.
30. Anaclet C, *et al*. Brainstem circuitry regulating phasic activation of trigeminal motoneurons during REM sleep. *PLoS One*. 2010;**5**(1):e8788.
31. Affanni J, *et al*. Higher nervous activity in cats with midpontine pretrigeminal transections. *Science*. 1962;**137**(3524):126–127.
32. Batini C, *et al*. Presistent patterns of wakefulness in the pretrigeminal midpontine preparation. *Science*. 1958;**128**(3314):30–32.
33. Fuller PM, *et al*. Reassessment of the structural basis of the ascending arousal system. *J Comp Neurol*. 2011;**519**(5):933–956.
34. Thakkar MM, *et al*. A1 receptor and adenosinergic homeostatic regulation of sleep-wakefulness: effects of antisense to the A1 receptor in the cholinergic basal forebrain. *J Neurosci*. 2003;**23**(10):4278–4287.